The RBBP6/ZBTB38/MCM10 Axis Regulates DNA Replication and Common Fragile Site Stability

Benoit Miotto, Moredreck Chibi, Ping Xie, Stéphane Koundrioukoff, Hanlie Moolman-Smook, David Pugh, Michelle Debatisse, Fuchu He, Lingqiang Zhang, Pierre-Antoine Defossez

Cell Reports
Article

The RBBP6/ZBTB38/MCM10 Axis Regulates DNA Replication and Common Fragile Site Stability

Benoit Miotto,[1,7] Moredreck Chibi,[1,2,7] Ping Xie,[3,4,7] Stéphane Koundrioukoff,[6] Hanlie Moolman-Smook,[5] David Pugh,[2] Michelle Debatisse,[6] Fuchu He,[3] Lingqiang Zhang,[3,4,*] and Pierre-Antoine Defossez[1,*]
[1]Epigenetics and Cell Fate, University Paris Diderot, Sorbonne Paris Cité, UMR 7216 CNRS, 75013 Paris, France
[2]Department of Biotechnology, University of the Western Cape, Bellville 7535, Republic of South Africa
[3]State Key Laboratory of Proteomics, Beijing Proteome Research Center, Beijing Institute of Radiation Medicine, Collaborative Innovation Center for Cancer Medicine, Beijing 100850, China
[4]Institute of Cancer Stem Cell, Dalian Medical University, Dalian, Liaoning Province 116044, China
[5]US/MRC Centre for Molecular and Cellular Biology, Department of Biomedical Sciences, University of Stellenbosch Health Sciences Faculty, Tygerberg 7600, Republic of South Africa
[6]Institut Curie, Centre de Recherche, and Sorbonne Universités, UPMC Université Paris 06, CNRS UMR, 324426 Rue d'Ulm, 75248 Paris, France
[7]These authors contributed equally to this work
*Correspondence: zhanglq@nic.bmi.ac.cn (L.Z.), pierre-antoine.defossez@univ-paris-diderot.fr (P.-A.D.)
http://dx.doi.org/10.1016/j.celrep.2014.03.030

SUMMARY

Faithful DNA replication is essential for the maintenance of genome integrity. Incomplete genome replication leads to DNA breaks and chromosomal rearrangements, which are causal factors in cancer and other human diseases. Despite their importance, the molecular mechanisms that control human genome stability are incompletely understood. Here, we report a pathway that is required for human genome replication and stability. This pathway has three components: an E3 ubiquitin ligase, a transcriptional repressor, and a replication protein. The E3 ubiquitin ligase RBBP6 ubiquitinates and destabilizes the transcriptional repressor ZBTB38. This repressor negatively regulates transcription and levels of the MCM10 replication factor on chromatin. Cells lacking RBBP6 experience reduced replication fork progression and increased damage at common fragile sites due to ZBTB38 accumulation and MCM10 downregulation. Our results uncover a pathway that ensures genome-wide DNA replication and chromosomal stability.

INTRODUCTION

Genomic instability underlies numerous human developmental disorders and diseases (Aguilera and Gómez-González, 2008). Its role has been particularly clearly shown in cancer, where genome instability contributes to both the appearance and heterogeneity of cancer (Burrell et al., 2013). Genome instability can arise from dysfunction in several surveillance and repair pathways, and DNA replication is a period during which the genome is especially vulnerable. Among the regions that are highly sensitive to replication abnormalities are common fragile sites (CFSs).

CFSs are regions of the genome that are especially sensitive to DNA replication stress and are likely to break under such conditions. A majority of cancer-related translocations contain breakpoints within CFSs, and many genes that have been identified as tumor suppressors or oncogenes are located at or within CFSs (Debatisse et al., 2012; Le Tallec et al., 2013; Ozeri-Galai et al., 2012), strongly arguing that CFS fragility contributes causally to cancer. For this reason and others, large research efforts have been directed toward understanding the biology of CFSs (Fungtammasan et al., 2012; Helmrich et al., 2011; Letessier et al., 2011). These investigations have led to the identification of a handful of DNA replication and DNA repair factors that influence CFS stability (Bergoglio et al., 2013; Koundrioukoff et al., 2013; Lukas et al., 2011; Naim et al., 2013; Ying et al., 2013). However, our understanding of CFS fragility is still far from complete.

In this study, we identify and characterize an essential pathway that opposes replication stress and CFS rearrangement. The upstream member of this pathway is the E3 ubiquitin ligase RBBP6. RBBP6 (also known as PACT or P2P-R) is an essential gene (Li et al., 2007) that encodes a protein that interacts with Rb, p53, and the pre-mRNA 3′ processing complex (Sakai et al., 1995; Shi et al., 2009; Simons et al., 1997), and whose expression is deregulated in human tumors (Chen et al., 2013; Mbita et al., 2012; Motadi et al., 2011; Yoshitake et al., 2004). Our experiments establish that RBBP6 regulates genomic replication and CFS stability, as in its absence DNA replication slows down and CFSs become lost from the genome. We show that RBBP6 fulfills this function by ubiquitinating a transcription factor, ZBTB38, and by promoting its degradation. Finally, we establish that the replication protein MCM10 is a direct target of transcriptional repression by

ZBTB38, and that its downregulation is responsible for the replication abnormalities that occur in the absence of RBBP6. These data further our understanding of genome stability and DNA replication, and provide evidence of a crucial role for the RBBP6/ZBTB38/MCM10 axis in genome perpetuation and stability.

RESULTS

Cells Lacking RBBP6 Experience Spontaneous DNA Damage

RBBP6 is an essential protein (Li et al., 2007) and is deregulated in cancer. This led us to investigate its function in mammalian cells. To that end, we depleted RBBP6 by RNAi in HeLa cells and monitored the cells for biological consequences. This phenotypic screening led us to observe that RBBP6-depleted cells showed signs of DNA damage, as evidenced by high levels of phospho-H2AX (or γH2AX), phosphorylated ATM, and phosphorylated Chk2 in western blots (Figure 1A). This effect was obtained with two independent small interfering RNA (siRNA) duplexes against RBBP6 (Figure S1A), it was rescued by the expression of a siRNA-resistant RBBP6 construct (Figure S1B), and it occurred in all of the other cell lines we tested (U2OS, Rb-depleted U2OS, HCT116, and HCT116 p53−/−; Figures S1C and S1D). To assess the percentage of cells in which damage occurred, we used immunofluorescence. These experiments showed that γH2AX foci were detectable in 39% of RBBP6-depleted cells, but in only 4% of control HeLa cells (Figure 1B). A similar proportion of these cells scored positively for the two other DNA damage markers that we tested: 53BP1 and Phospho-S1524-BRCA1 (Figures 1C and S1E). Finally, the effect of RBBP6 was not restricted to cancer cell lines, as the depletion of RBBP6 caused the spontaneous appearance of DNA damage in normal human fibroblasts as well (Figures 1D and S1F). These data indicate that RBBP6 function is required to prevent DNA damage.

DNA Damage Associated with RBBP6 Depletion Is Prevented by Simultaneous Depletion of the Transcriptional Repressor ZBTB38

We previously conducted a yeast two-hybrid screen to identify possible interactors of RBBP6 (Chibi et al., 2008); therefore, we tested whether any of these candidates was required for the phenotypes seen upon RBBP6 knockdown. We found that the RNAi depletion of ZBTB38 completely suppressed the elevated levels of all DNA damage indicators (Figures 1A–1D) that had been caused by RBBP6 knockdown, and this was true both in cancer cells and in normal human fibroblasts. Importantly, by itself, ZBTB38 depletion had no detectable effect in any of our tests (Figures 1A–1D). We considered the possibility that rather than preventing DNA damage, ZBTB38 knockdown might have merely prevented the activation of signaling pathways. To test this possibility, we submitted ZBTB38-depleted cells to a challenge with the replication inhibitor Aphidicolin, which causes DNA damage. We found that these cells had levels of ATM and Chk2 phosphorylation identical to those observed in control cells, which establishes that they are not defective for DNA damage signaling (data not shown). Therefore, we conclude that the DNA damage that occurs upon RBBP6 knockdown is fully prevented when ZBTB38 is simultaneously depleted. This strong genetic interaction suggests that the two proteins function in the same pathway to prevent DNA damage.

We next tested the involvement of other partners of RBBP6, including p53, Rb, and the pre-mRNA processing complex (Sakai et al., 1995; Shi et al., 2009; Simons et al., 1997). By western blotting, we observed that depletion of RBBP6 caused DNA damage in cells inactivated for p53 (HCT116 versus HCT116 p53−/− cells; Figure S1D), in cells depleted for Rb (Figure S1D), and in cells overexpressing RNase H1, which degrades RNA/DNA duplexes produced by defective mRNA processing (Figures S1G and S1H). These observations argue that the primary cause of DNA damage in cells depleted of RBBP6 is ZBTB38 dependent.

Cells Lacking RBBP6 Have Higher Levels of ZBTB38 Protein, and Overexpression of ZBTB38 Is Sufficient to Induce DNA Damage

We next investigated the molecular link between ZBTB38 and RBBP6. By western blotting, we observed an ~3-fold increase in the ZBTB38 protein level in HeLa cells depleted of RBBP6 relative to control cells (Figures 1A, 2A, and S2A). In contrast, ZBTB4 (a paralog of ZBTB38) and Rb (a potential RBBP6 interactor (Simons et al., 1997)) were unaffected (Figures 2A and S2A). A similar increase in the ZBTB38 protein level in cells treated with RBBP6-specific siRNAs was observed in all of the other cell lines we tested (3.4- to 5.4-fold increase in different cell types; Figure 2B) and was also seen with an independent ZBTB38 antibody (Figure S2A). We therefore conclude that in the absence of RBBP6, ZBTB38 protein levels are higher in cells and that this coincides with DNA damage.

This observation led us to speculate that the increase in ZBTB38 expression might directly cause DNA damage. We thus overexpressed ZBTB38 in HeLa and U2OS cells and monitored DNA damage. By western blotting, we observed high levels of γH2AX and phosphorylated Chk2 in both cell types (Figure 2C). Thus, the overexpression of ZBTB38 is sufficient to cause DNA damage and its depletion is sufficient to prevent DNA damage in the absence of RBBP6. It is therefore highly likely that the accumulation of ZBTB38 is the primary cause of DNA damage in cells depleted of RBBP6.

RBBP6 Ubiquitinates the ZBTB38 Protein and Controls its Stability

We investigated how RBBP6 regulates ZBTB38 abundance to prevent DNA damage. The level of *ZBTB38* mRNA was not increased after RBBP6 knockdown (Figure S2B), arguing that the upregulation was primarily posttranscriptional. RBBP6 contains a RING finger domain (Kappo et al., 2012), which is often associated with an E3 ubiquitin ligase activity and protein destabilization. This led us to test whether RBBP6 was regulating ZBTB38 protein stability. By performing coimmunoprecipitation (coIP) on nuclear extracts, pull-down experiments, and a subnuclear recruitment assay, we first established that the two proteins interact (Figure S3). We next measured the half-life of endogenous ZBTB38 and found that it was greatly increased

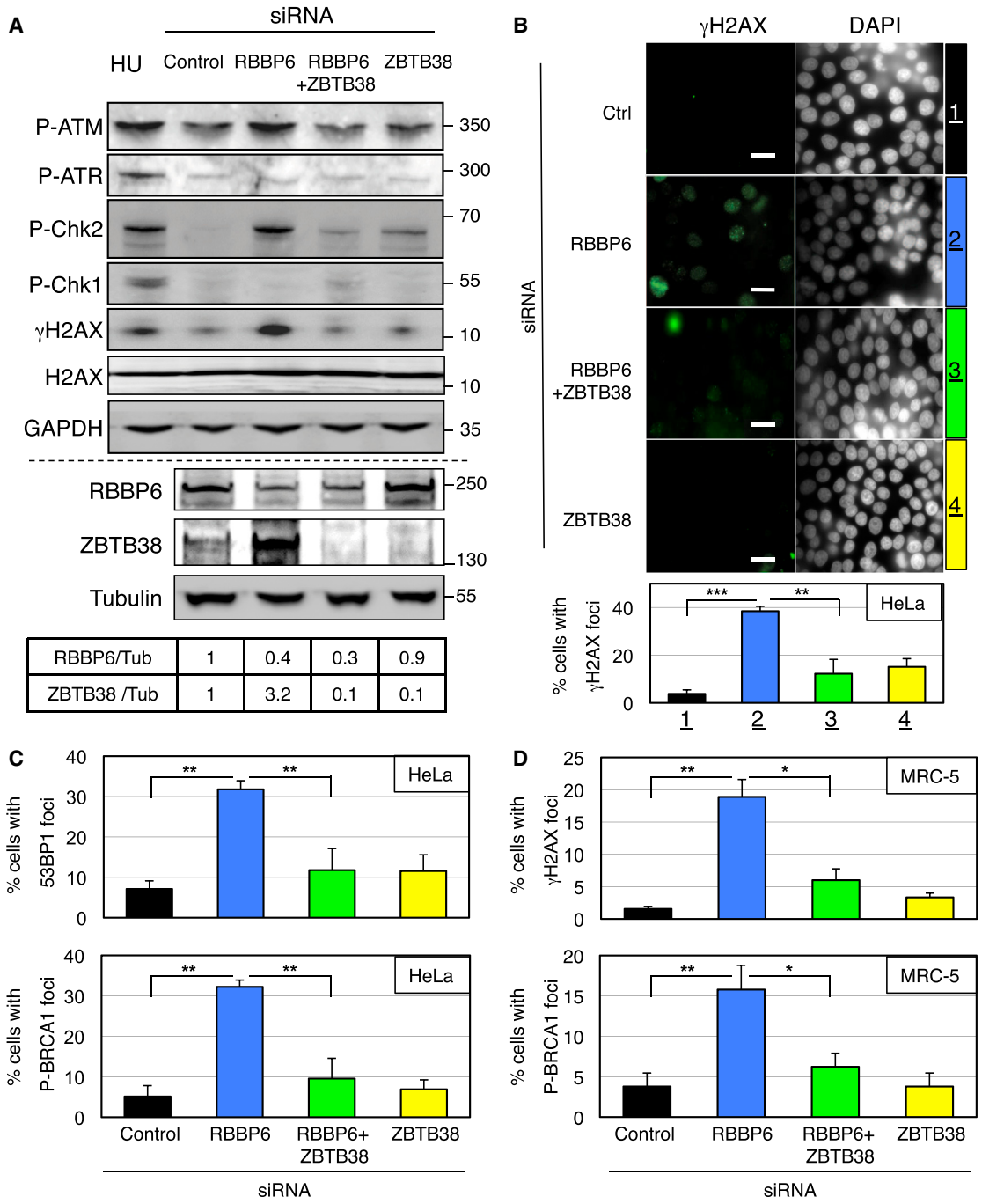

Figure 1. Depletion of RBBP6 Causes DNA Damage, which Is Rescued by Simultaneous ZBTB38 Depletion

(A) The depletion of RBBP6 by RNAi causes the appearance of phosphorylated histone H2AX and an increase of ATM and Chk2 phosphorylation, but not ATR or Chk1 phosphorylation. This effect is prevented by the simultaneous depletion of ZBTB38. Extracts of cells transfected with the indicated siRNA duplexes were used for western blotting. "P-" denotes the phosphorylated form of the different proteins assayed. Treatment with HU (2 mM, 16 hr) was used as a positive control of damage induction.

(B) Analysis of damage on a cell-by-cell basis. HeLa cells were transfected with the indicated siRNAs and fixed 48 hr after transfection. They were then processed for immunofluorescence with an antibody against γH2AX, and the nuclei were counterstained with DAPI. For quantification of (B)–(D), we scored 150 cells for each condition in three independent experiments.

(C) The presence of 53BP1 or P-BRCA1 foci was scored as in (B).

(D) RBBP6 depletion causes DNA damage in normal human fibroblasts, and this is rescued by simultaneous ZBTB38 depletion. The same procedure as in (B) and (C) was used, but the experiment was performed on MRC-5 cells. In all figures: *$p < 0.05$, **$p < 0.01$, ***$p < 0.001$; NS, no statistical significance.

See also Figure S1.

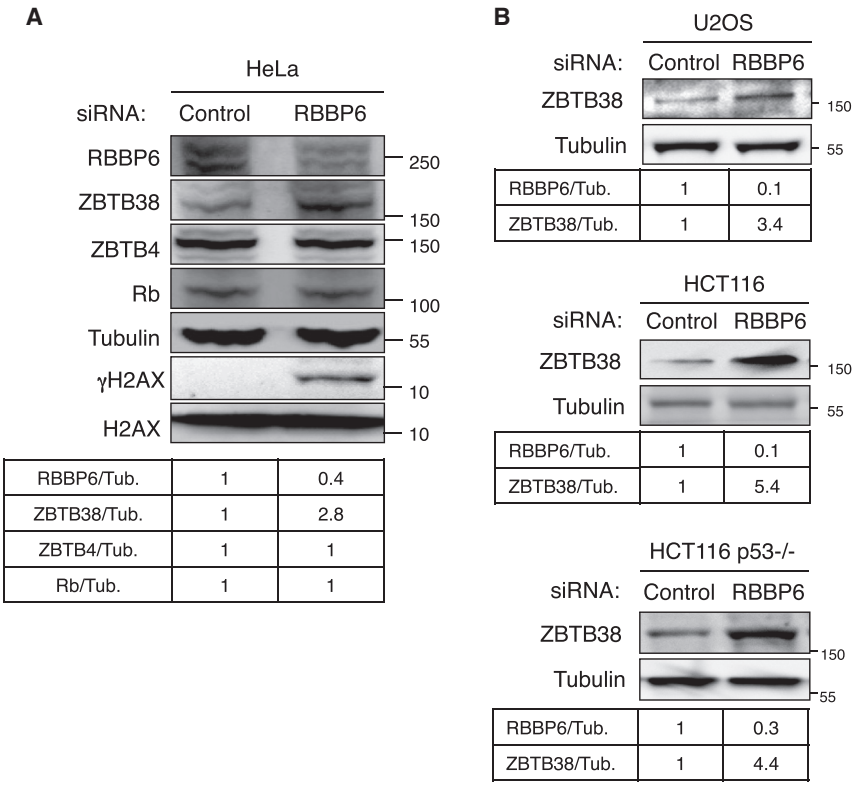

RBBP6/Tub.	1	0.4
ZBTB38/Tub.	1	2.8
ZBTB4/Tub.	1	1
Rb/Tub.	1	1

Figure 2. Depletion of RBBP6 Causes an Increase in the ZBTB38 Protein Level, and Overexpression of ZBTB38 Is Sufficient to Cause DNA Damage

(A) RBBP6 depletion does not affect ZBTB4 or Rb abundance in HeLa cells, but increases the ZBTB38 protein level. HeLa cells were transfected with siRNA duplexes targeting *RBBP6* or with a scrambled control siRNA. Cell extracts were then used for immunoblotting with the indicated antibodies. Quantitation shows the ratio of signal relative to tubulin (Tub.) for each indicated protein.

(B) Western blot analysis of ZBTB38 protein level in the three indicated cell types transfected with control siRNA or with siRNA targeting RBBP6.

(C) Overexpression of ZBTB38 causes DNA damage. HeLa cells or U2OS cells were transfected with a plasmid encoding ZBTB38 and 48 hr later, cell extracts were used for immunoblotting with the indicated antibodies.

See also Figure S2.

(going from 4 hr to >12 hr) after RBBP6 knockdown (Figure 3A). Therefore, the loss of endogenous RBBP6 after RNAi increased ZBTB38 protein stability. Conversely, the overexpression of RBBP6 led to a large decrease in the level of endogenous ZBTB38 that was detectable by immunofluorescence, and this effect was prevented by inhibiting the proteasome with MG132 (Figure 3B). The regulation was specific, as the overexpression of RBBP6 did not detectably affect ZBTB4 (Figure 3B). Thus, RBBP6 induces ZBTB38 protein degradation, and this depends on the activity of the proteasome.

We next tested whether RBBP6 might directly ubiquitinate ZBTB38. We showed that the knockdown of RBBP6 decreased the amount of ubiquitinated ZBTB38 in cells (Figure 3C). Conversely, the overexpression of RBBP6 led to ZBTB38 ubiquitination in cells (Figure 3D). This effect of RBBP6 on ZBTB38 is also observed in the absence of MDM2 in mouse embryonic *p53−/− Mdm2−/−* cells (data not shown) and therefore is distinct from the mechanism used to regulate p53 stability, which is MDM2 dependent (Li et al., 2007).

Finally, we set up an in vitro reconstituted system. The E2 for RBBP6 is unknown; however, the RING finger of RBBP6 is structurally related to that of Bmi1 and Ring1B (Kappo et al., 2012), and UbcH5c functions an E2 ligase for these proteins (Buchwald et al., 2006), so we hypothesized it might do the same for RBBP6. We found that RBBP6 drove the ubiquitination of RFP-ZBTB38 in vitro in the presence of UbcH5c, whereas a ΔRING mutant of RBBP6 had no such effect (Figure 3E). Together, these data show that RBBP6 functions as an E3 ligase to promote the ubiquitination and proteasomal degradation of ZBTB38.

Cells Lacking RBBP6 Show Increased Chromosomal Instability and Evidence of Underreplication of the Genome, which Is Rescued by Simultaneous Codepletion of ZBTB38

We next monitored different aspects of DNA maintenance in the RBBP6-depleted cells. We noticed that upon RBBP6 depletion, a significant increase occurred in the level of DNA bridges and PICH-positive bridges (Figures 4A and 4B) during anaphase. These bridges are indicative of cells entering M phase with

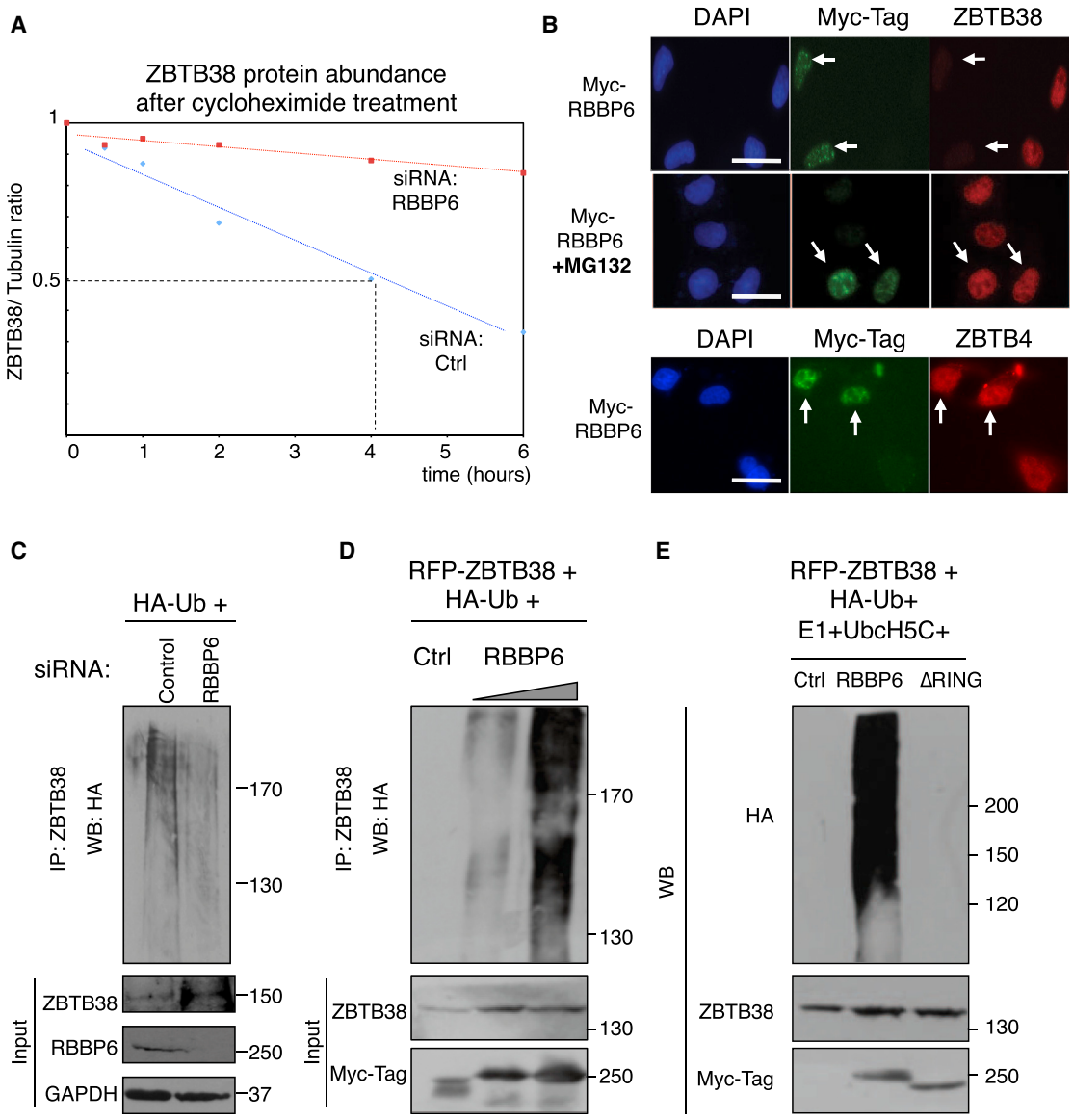

Figure 3. RBBP6 Decreases ZBTB38 Protein Stability and Abundance via Ubiquitination and Proteasomal Degradation

(A) Depletion of RBBP6 prolongs the half-life of endogenous ZBTB38 protein. HeLa cells were transfected with a siRNA duplex targeting *RBBP6* or with a scrambled control duplex (Ctrl). The cells were then treated with cycloheximide and extracts were collected at the indicated time intervals (in hours). The ratio of ZBTB38 to tubulin signals in the samples is displayed, with the t = 0 time point set as 1.

(B) RBBP6 overexpression leads to proteasomal degradation of ZBTB38, but not ZBTB4. HeLa cells were transfected with an expression vector for Myc-RBBP6 and then subjected to immunofluorescence with the indicated antibodies. The arrows indicate the position of cells expressing Myc-tagged proteins. Scale bar, 25 μm.

(C) Endogenous RBBP6 controls the ubiquitination of ZBTB38. HeLa cells were transfected with a plasmid expressing hemagglutinin (HA)-tagged ubiquitin, along with a siRNA targeting *RBBP6* or a scrambled control siRNA. The cells were treated with MG132, and extracts were processed by IP and western blotting as indicated. After RBBP6 knockdown, there was a decrease in the amount of ubiquitinated ZBTB38.

(D) RBBP6 promotes the polyubiquitination of ZBTB38 in cells. HeLa cells were transfected with the indicated plasmid combinations and treated with MG132. Cell extracts were processed by IP and western blotting (WB) as indicated. The overexpression of RBBP6 led to the appearance of ubiquitin conjugates on ZBTB38.

(E) RBBP6 promotes the polyubiquitination of ZBTB38 in vitro. RFP-ZBTB38 was immunoprecipitated from transfected cells and incubated with purified E1 (Uba1), HA-tagged ubiquitin, the E2 conjugating enzyme UbcH5C, and wild-type Myc-tagged RBBP6 (WT) or its RING-deleted derivative (ΔR) immunoprecipitated from transfected cells. The reaction products were probed by western blotting with an HA antibody to detect ubiquitin conjugates.

See also Figure S3.

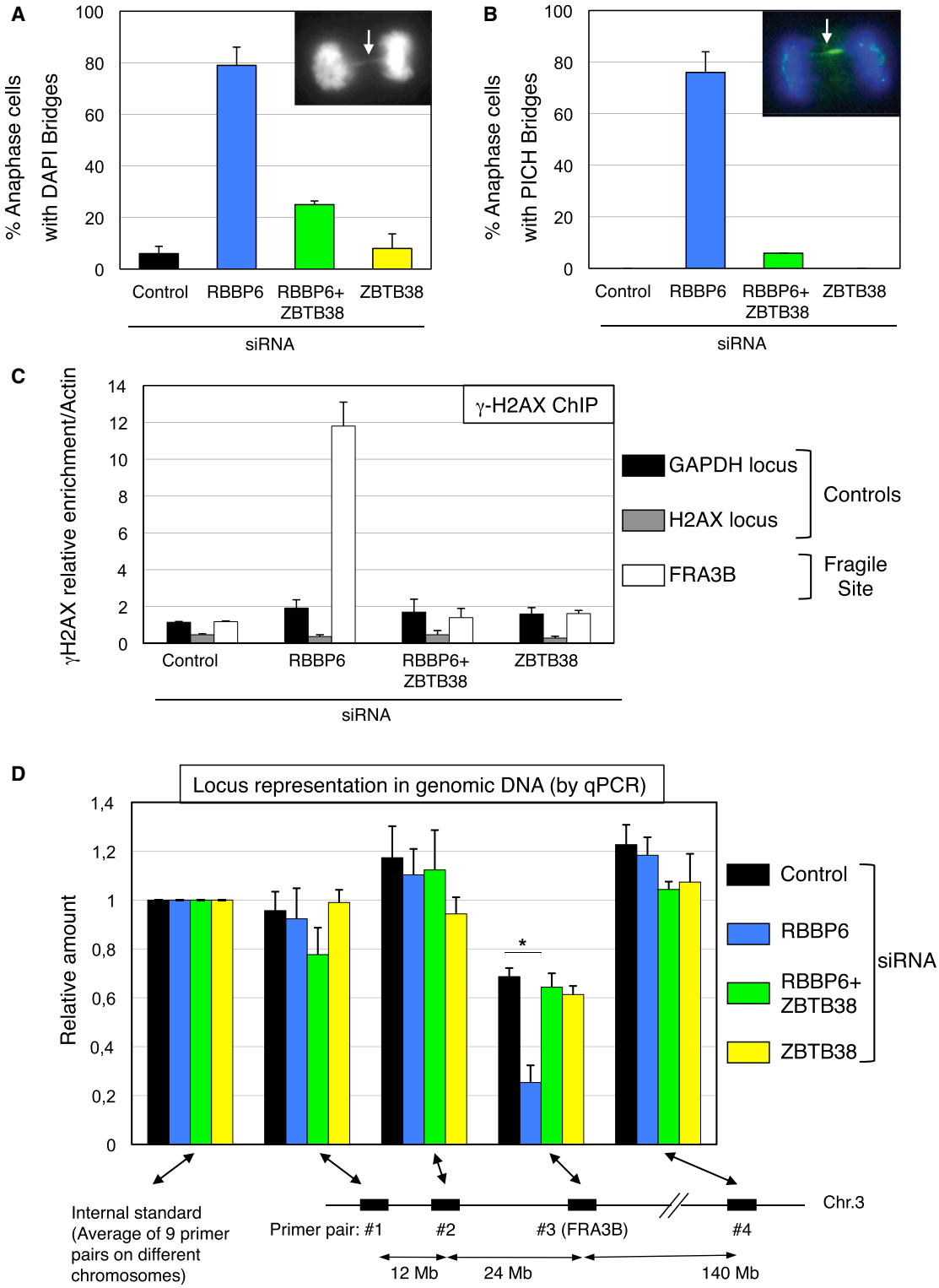

Figure 4. RBBP6 and ZBTB38 Control the Integrity and Stability of a CFS

(A) Cells depleted of RBBP6 frequently present DAPI bridges in anaphase. Quantification of the phenotype in HeLa cells transfected with the indicated siRNA combinations, and the average and SD from 150 cells in each of three independent experiments are shown. Inset: a representative anaphase cell that scored positive for the presence of a DAPI bridge (arrow).

(legend continued on next page)

regions of the genome being incompletely replicated (Chan and Hickson, 2009). CFSs are often found in these regions, and we thus hypothesized that they could be affected by RBBP6 depletion. By performing chromatin IP (ChIP) for γH2AX, we observed that the FRA3B/FHIT locus, a CFS, indeed bore the mark of DNA damage in RBBP6 knockdown cells (Figure 4C), whereas the two control loci we examined did not. This establishes that RBBP6 is necessary to prevent the occurrence of damage at the FRA3B/FHIT locus. In addition, using a PCR-based assay, we observed loss of the FRA3B sites in a population of HeLa cells depleted of RBBP6 (Figure 4D). We next tested whether the genomic instability was specific to the FRA3B fragile site. In U2OS cells, we observed increased breakage at the FRA3B and FRA16 fragile sites upon RBBP6 depletion (Figure S4A), indicating that the effect of RBBP6 is not restricted to a single CFS or a single cell type.

To gain more insight into the underlying mechanism, we also investigated an artificial fragile region. It was recently reported that LacOp arrays are prone to missegregation in the presence of LacR, and this phenomenon is enhanced in conditions that promote replication stress and fragile site breakage (Jacome and Fernandez-Capetillo, 2011). We thus monitored the number of LacR spots in mouse 3T3 cells harboring integrated LacOp arrays (Soutoglou and Misteli, 2008), expressing a Cherry-LacR fusion construct, and depleted of RBBP6. We observed an increased number of cells with no LacR spots or more than one spot, and conversely a diminution of the cells with a single spot (Figures S4B and S4C). This reflects missegregation of the LacOp repeats in the absence of RBBP6 and proves that RBBP6 is essential for the stability of this artificial fragile region. Altogether, these results indicate that RBBP6 is required for chromosome stability and that inactivation of RBBP6 leads to chromosomal breakage at genomic sites susceptible to replication stress, such as CFSs, in mouse and human cells.

We next investigated whether chromosomal instability was also rescued by ZBTB38 depletion. Again the RNAi depletion of ZBTB38 by itself had no detectable effect in any of these tests (Figure 4). In striking contrast, the ZBTB38 knockdown suppressed (1) the presence of anaphase bridges (Figures 4A and 4B), (2) the presence of damage at CFSs (Figure 4C), (3) the chromosomal instability at CFSs (Figure 4D and S4A), and (4) the missegregation of LacOp arrays (Figure S4C). In summary, all of the phenotypes seen upon RBBP6 knockdown are rescued if ZBTB38 is simultaneously depleted.

RBBP6 Regulates Replication Fork Speed and Interorigin Distance in a ZBTB38-Dependent Manner

The presence of underreplicated DNA in the absence of RBBP6 led us to investigate how RBBP6 regulates DNA replication and how ZBTB38 accumulation perturbed this regulation. First, we monitored the viability of RBBP6-depleted cells exposed to low doses of hydroxyurea (HU), a replication inhibitor (Arlt et al., 2011). These low doses were not toxic to control cells, but killed 40% of the RBBP6 knockdown cells (Figure 5A). Treatment with mitomycin C, another drug that impedes DNA replication (Sognier and Hittelman, 1986), was also much more toxic to RBBP6-depleted than to control cells (Figure 5B). These experiments show that cells lacking RBBP6 are hypersensitive to a replication challenge.

We next investigated whether cells depleted of RBBP6 present DNA replication stress. The defects that uncouple the helicase and polymerase activities of the replisome lead to the formation of single-strand DNA, which can then be detectable by bromodeoxyuridine (BrdU) staining in the absence of DNA denaturation (Koundrioukoff et al., 2013) and by the formation of phospho-RPA32 foci (Sirbu et al., 2011). HU treatment caused both marks to occur, whereas RBBP6 depletion did not trigger either one (Figure S5A). Therefore, RBBP6 depletion does not lead to the formation of detectable levels of single-strand DNA, arguing that depletion of RBBP6 causes a mild replication defect and/or that compensation mechanisms exist.

We directly tested the function of RBBP6 in DNA replication by using DNA combing (Técher et al., 2013). RBBP6 was silenced in U2OS cells, and following 5-iodo deoxy uridine (IdU) and 5-chloro-2′-deoxyuridine (CldU) pulses, we calculated the distances between replication origins (in origin clusters), fork velocities, and asymmetry. In cells treated with RBBP6 siRNA, we observed a significant decrease in replication fork speed compared with control (Figure 5C). We also observed that the interorigin distance in clusters was significantly lower (Figure 5D). In contrast, loss of RBBP6 in cells had no effect on replication fork stalling and/or collapse, and there was no asymmetry in fork progression (Figure S5B and data not shown). Thus, depletion of RBBP6 causes a reduction in fork progression coincident with endogenous replication stress and chromosomal instability. However, interorigin distance also was reduced, which partially compensated for the reduction in fork speed.

Again we investigated whether DNA replication defects were rescued by ZBTB38 depletion. The RNAi depletion of ZBTB38 by itself had no detectable effect in any of these tests (Figures 5A–5D), but in striking contrast, the ZBTB38 knockdown suppressed (1) the hypersensitivity to HU and Mitomycin C (Figures 5A and 5B), (2) the decreased speed of replication forks (Figure 5C), and (3) the decreased interorigin distance (Figure 5D). In summary, all of the phenotypes seen upon RBBP6 knockdown were rescued when ZBTB38 was simultaneously depleted.

We thus conclude from these experiments that RBBP6 regulates DNA replication. In the absence of RBBP6, ZBTB38

(B) Cells depleted of RBBP6 frequently present PICH-covered bridges in anaphase. Quantification of the phenotype in HeLa cells transfected with the indicated siRNA combinations, and the average and SD from 150 cells in each of three independent experiments are shown. Inset: a representative anaphase cell that scored positive for the presence of a PICH bridge (arrow). PICH staining is represented in green, overlaid on the DAPI staining (blue).
(C) RBBP6-depleted cells suffer DNA damage at the *FRA3B/FHIT* fragile site, and this is suppressed by simultaneous ZBTB38 depletion. Cells were transfected with the indicated siRNAs and then the presence of γH2AX at the three indicated loci was tested by ChIP.
(D) The *FRA3B* locus becomes underrepresented in a cell population after RBBP6 depletion. After siRNA transfection, total genomic DNA was extracted and the abundance of *FRA3B* and other loci along chromosome 3 was measured by qPCR. Internal standard: average of nine loci located on other chromosomes. Average and SD from two biological replicates, each with technical triplicates.
See also Figure S4.

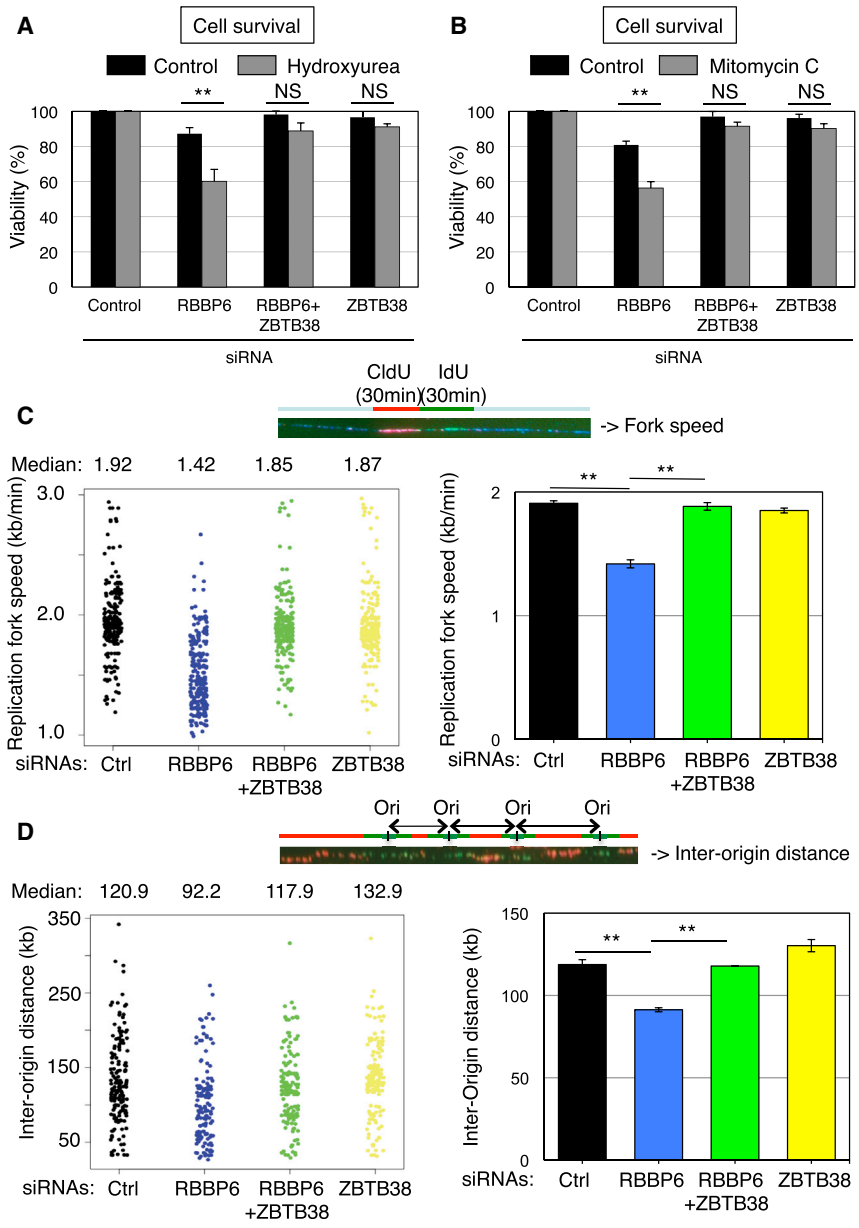

Figure 5. RBBP6 Regulates DNA Replication in a ZBTB38-Dependent Manner

(A) RBBP6-depleted cells are hypersensitive to low doses of HU. After transfection with the indicated siRNAs, HeLa cells were treated with a low dose of HU (200 μM for 16 hr) and then viability was assessed by trypan blue exclusion.

(B) As in the previous panel, except that the cells were treated with Mitomycin C (1 μg/ml for 12 hr).

(C) RBBP6 depletion reduces replication fork speed. U2OS cells were transfected with the indicated siRNAs for 48 hr and then labeled with IdU (30 min) and CldU (30 min) and prepared for single-molecule DNA fiber analysis. A representative DNA fiber from control siRNA-treated cells is provided. Left panel: distribution of replication fork velocities in a representative experiment. A total of 150 replication forks were analyzed per condition and the median speed value is indicated on top of each bar. Right panel: the average of the median replication fork velocity for each siRNA condition was calculated from three independent experiments (150 forks per condition were analyzed in each single experiment).

(D) RBBP6 depletion reduces the interorigin distance (IOD) in replication origin clusters. A representative DNA fiber from control siRNA-treated cells is provided. Left panel: distribution of IODs in a representative experiment. A total of 150 fibers were analyzed per siRNA condition and the median value is indicated on top of each bar. Right panel: the average of the median IOD for each siRNA condition was calculated in two independent experiments (150 fibers were analyzed per siRNA condition).

See also Figure S5.

is overabundant, and this leads to an altered program of DNA replication and chromosomal instability.

The Replication Factor MCM10 Is a Target of RBBP6 and ZBTB38, and Mediates Most of the Effects of RBBP6 and ZBTB38

We next wanted to identify the role of RBBP6 and ZBTB38 in DNA replication regulation. By western blotting on chromatin fractions, we examined the loading of different DNA repair and replication factors onto the chromatin. We found that DNA damage response factors (BRCA1 and TOPBP1) and γH2AX binding onto the chromatin was strongly enhanced in the absence of RBBP6, consistent with the presence of DNA damage in the cells (Figure 6A). The amounts of prereplication complex components (ORC2, MCM3, CDT1, and HBO1/KAT7) associated with the chromatin were similar in RBBP6-depleted and control cells (Figure 6A), ruling out an effect of RBBP6 on prereplication complex (preRC) loading. The amounts of the DNA replication clamp PCNA, the specialized DNA polymerase POLH/XPV, and the mini-chromosome maintenance subunit 7 (MCM7) associated with the chromatin were similar in RBBP6-depleted and control cells (Figure 6A). In contrast, we detected a significantly lower amount of MCM10, a factor involved in DNA replication activation (Kanke et al., 2012; van Deursen et al., 2012; Watase et al., 2012; Zhu et al., 2007), in RBBP6-depleted cells compared with control (Figure 6A). These observations indicate that the DNA replication factor MCM10 is not properly associated with chromatin in cells depleted of RBBP6. This effect is eliminated if ZBTB38 is depleted along with RBBP6 (Figure 6A).

These results raised the possibility that decreased MCM10 abundance and/or loading was responsible for the phenotypes observed in RBBP6-depleted cells. To test this possibility, we depleted MCM10 by RNAi and repeated the functional assays described above. We found that the depletion of MCM10 caused

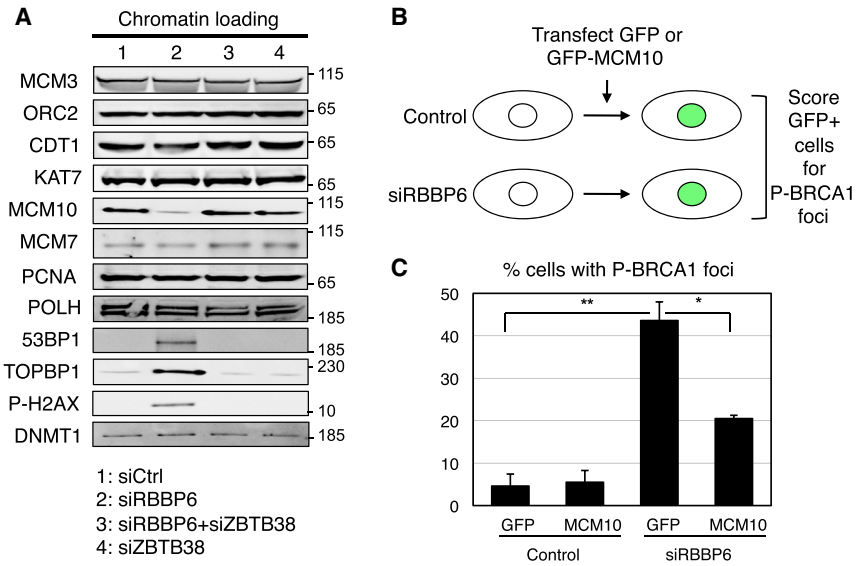

Figure 6. MCM10 Is Affected by RBBP6 Depletion, and Overexpression of MCM10 Rescues DNA Damage Caused by RBBP6 Depletion

(A) RBBP6 depletion coincides with lower amounts of MCM10 protein loaded onto chromatin. HeLa cells were transfected with the indicated siRNA duplexes. Chromatin fractions (nuclease-resistant fractions) were then prepared and the amount of the indicated chromatin-bound nuclear factors was analyzed by western blot.

(B) MCM10 reexpression suppresses DNA damage in cells depleted of RBBP6. Design of the rescue experiment with GFP-MCM10.

(C) Graph representing the percentage of cells that exhibited phospho-BRCA1 foci in the different siRNA conditions (n = 100 in each of 3 independent experiments).

See also Figure S6.

spontaneous DNA damage (Figures S6A and S6B), ATM and Chk2 activation (Figure S6A), hypersensitivity to HU and MMC (Figure S6C), the appearance of frequent PICH-positive anaphase bridges (Figure S6D), loss of *FRA3B* and *FRA16* in U2OS cells (Figure S6E), missegregation of LacO repeats (Figure S6F), and a significant reduction of DNA replication fork speed and interorigin distance (Figure S6G). Therefore, MCM10 depletion causes similar phenotypes as RBBP6 depletion, arguing that it could be a relevant functional target.

To test this hypothesis experimentally, we set up a rescue assay. In this experiment, we reintroduced expression plasmids for tagged proteins in cells that had undergone siRNA depletion of RBBP6. We then used immunofluorescence to assess the presence of DNA damage in the transfected cells. Our control experiment showed that, as expected, the reexpression of RBBP6 rescued the effects of RBBP6 siRNA. Importantly, we observed that the percentage of cells bearing P-BRCA1 foci after RBBP6 depletion was decreased 2-fold by simultaneous transfection of an MCM10 expression vector (Figures 6B and 6C). This phenotypic rescue establishes that MCM10 is an important target that links the loss of RBBP6 to DNA damage.

The Replication Factor MCM10 Is a Transcriptional Target of RBBP6 and ZBTB38

We next investigated how ZBTB38 stabilization in cells lacking RBBP6 might affect MCM10 function. Since ZBTB38 is a transcriptional repressor (Filion et al., 2006; Sasai et al., 2005), we monitored the expression of MCM10 protein and mRNA (Figures 7A, 7B, and S7). In the three cell types tested, MCM10 was repressed by RBBP6 knockdown at the protein and mRNA levels (Figures 7A, 7B, and S7B). It was reexpressed upon simultaneous ZBTB38 knockdown (Figures 7A, 7B, and S7B). Other replication factors used as controls did not show any such variation, ruling out indirect consequences of a possible cell-cycle alteration caused by the knockdowns (Figures 7A, 7B, S7A, and S7B).

Is the downregulation of *MCM10* after RBBP6 depletion (and the occurrence of damage) merely a response to activated DNA damage signaling pathways? This is unlikely, as we observed the downregulation even in the presence of caffeine (Figure 7C) or KU55933 (data not shown), both of which block DNA damage signaling. Thus, our data indicate that ZBTB38 accumulation represses *MCM10* transcription, causing a subsequent decrease in MCM10 protein level.

We then asked whether ZBTB38 directly repressed the expression of *MCM10*. First, we used luciferase reporter constructs. In this assay, ZBTB38 repressed transcription from the *MCM10* promoter, but did not affect control promoters (Figure 7D). Second, we showed by ChIP that the *MCM10* promoter was bound by ZBTB38 in cells (Figure 7E). Third, we overexpressed ZBTB38 in HeLa cells and monitored endogenous MCM10 mRNA and protein expression. We observed that expression of ZBTB38 was sufficient to cause a decrease in MCM10 mRNA and protein expression (Figures 7F and 7G)

These results establish a direct and causal link between elevated ZBTB38 levels, MCM10 downregulation, and the appearance of DNA damage (model presented in Figures S7C–S7E).

DISCUSSION

We report that the human E3 ligase RBBP6 and the transcriptional repressor ZBTB38 are essential for genome replication, perpetuation, and stability. Previous work linked RBBP6 to p53 (Simons et al., 1997), but genetic evidence argued that it had important targets aside from p53 (Li et al., 2007). Our experiments identify the Zinc finger protein ZBTB38 as a key effector of RBBP6. When RBBP6 is depleted, ZBTB38 accumulates (Figure 2), and this causes DNA damage, a reduction in DNA replication fork speed, CFS underreplication, and chromosome segregation defects (Figures 1 and 4). We show that ZBTB38 is directly ubiquitinated by RBBP6 in human and mouse cells, in a process that is independent of p53 and MDM2, and leads to proteasomal degradation (Figure 3). We identify an RBBP6 target in cells, as

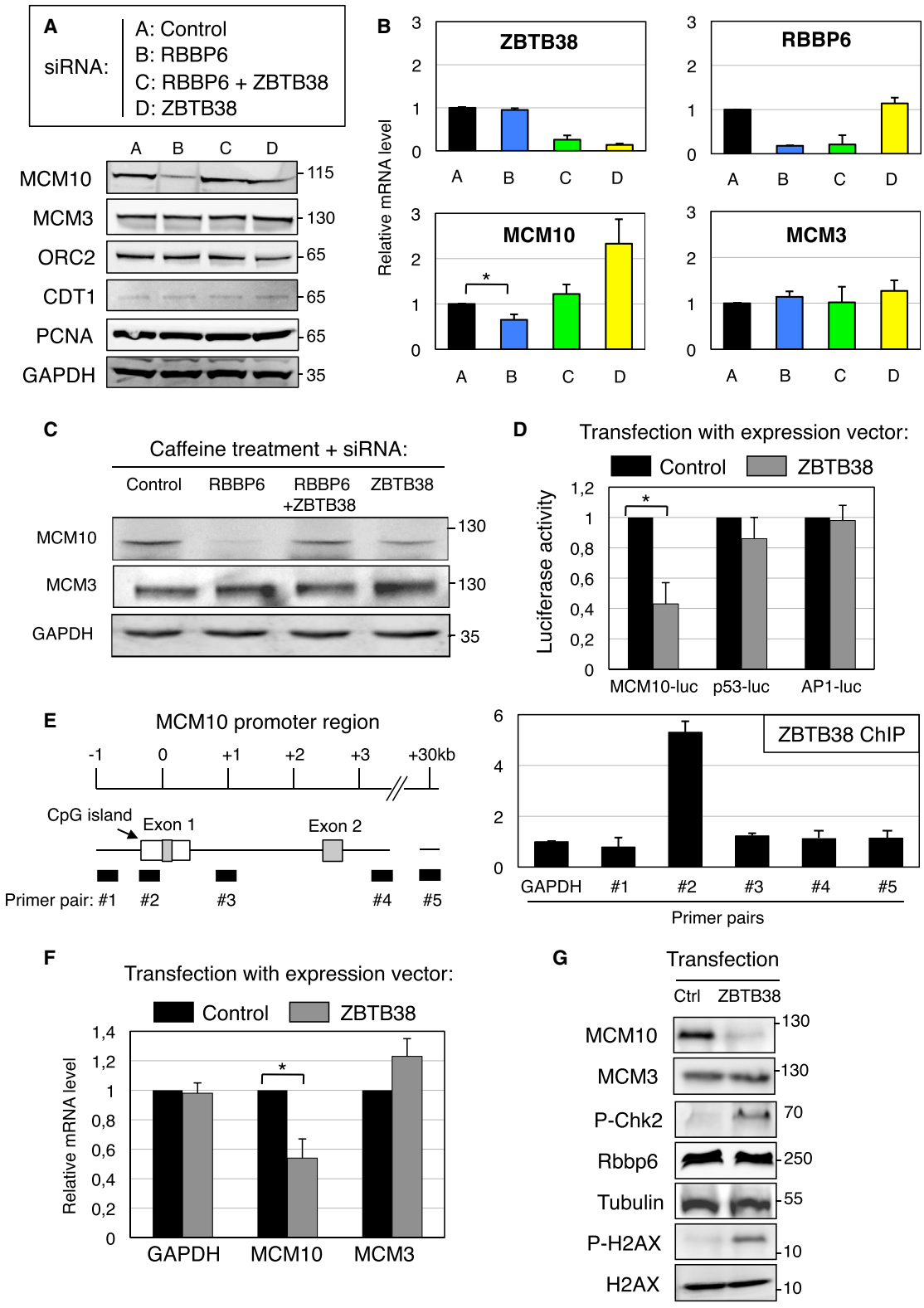

Figure 7. RBBP6 and ZBTB38 Regulate the Expression of Replication Factor MCM10

(A) The MCM10 protein is depleted following RBBP6 knockdown, but its level is normal if ZBTB38 is simultaneously removed. Other replication factors (e.g., MCM3, ORC2, CDT1, and PCNA) do not follow this trend. Extracts of cells transfected with the indicated siRNA duplexes were used for western blotting.

(legend continued on next page)

well as a ZBTB38 regulator. We note that a proteome-wide study identified lysines 112 and 804 of ZBTB38 as polyubiquitin acceptor sites (Kim et al., 2011). This supports the idea that ZBTB38 is regulated by ubiquitination, and raises the possibility that these sites are targets of RBBP6.

We have also identified MCM10 as a key effector of the RBBP6/ZBTB38 axis. Expression of MCM10 in RBBP6-depleted cells prevents DNA damage (Figure 6), MCM10 depletion causes similar phenotypes as RBBP6 depletion (Figure S6), and elevated levels of ZBTB38 lead to *MCM10* repression (Figure 7). ZBTB38 is a bifunctional transcriptional repressor that can bind methylated DNA as well as certain nonmethylated consensus sites (Sasai et al., 2010). We believe the latter mode of binding underlies the regulation of *MCM10*. First, ZBTB38 inhibits the expression of a *MCM10* luciferase reporter plasmid, which is devoid of CpG methylation because of its bacterial origin (Figure 7D). Second, the *MCM10* promoter is a CpG island, and these elements are generally methylation free in cells (Figure 7E). Third, we found a potential nonmethylated ZBTB38 consensus motif, TGCCA, at −84 bp from the transcription start site of *MCM10*. For these reasons, we believe the regulation of MCM10 by ZBTB38 is methylation independent.

MCM10 is unequivocally required for DNA replication in eukaryotes (Kanke et al., 2012; van Deursen et al., 2012; Watase et al., 2012; Zhu et al., 2007), yet its molecular roles are still a matter of debate (Thu and Bielinsky, 2013). The phenotypes we observe in the absence of RBBP6 or in the absence of MCM10 are identical and characterized by slow replication fork progression, decreased interorigin distance, and the presence of DNA damage. This occurs in the absence of detectable RPA32 foci and ATR/Chk1 activation (Figures 1A and S5A). These phenotypes are compatible with the proposed role of MCM10 in promoting replication elongation (Thu and Bielinsky, 2013). The simplest model for cells lacking RBBP6 (or overexpressing ZBTB38) is that the lowered MCM10 level results in a mildly defective DNA replication program in which slower replication forks fail to meet at certain sensitive chromosomal regions. Such underreplicated loci do not necessarily cause checkpoint activation, but can subsist through the G2 phase, be converted to lesions during mitosis, and be incorporated into 53BP1 foci to be repaired during the following G1 (Chan and Hickson, 2009; Harrigan et al., 2011; Lukas et al., 2011). The effects we observe upon RBBP6 depletion are all consistent with such a scenario occurring in chromosomal regions that are susceptible to replication stress, and in particular CFSs.

This simple model, of course, does not exclude other possible roles of MCM10. We previously showed that simply decreasing fork speed by 25% with low doses of HU was not sufficient to generate DNA damage, at least in U2OS cells (Domínguez-Kelly et al., 2011). Therefore, it is possible that in cells with low MCM10, another molecular defect compounds the problems caused by the slow replication speed. A possible candidate is altered DNA repair. Indeed, accumulating evidence suggests that MCM10 functions in DNA repair in association with TOPBP1 (Balestrini et al., 2010; Germann et al., 2011; Im et al., 2009; Kumagai et al., 2010; Tanaka et al., 2013; Taylor et al., 2011; Wawrousek et al., 2010; Yoshida and Inoue, 2004). The importance of efficient DNA repair for CFS stability is underlined by the fact that many of the genetic alterations that are known to cause breaks at CFS reportedly affect genes that code for DNA repair factors such as POLeta (Bergoglio et al., 2013), BRCA2, RAD51, TOPBP1, and TOP2A (Lukas et al., 2011). Irrespective of whether MCM10 acts by regulating DNA replication, DNA repair, or both, our data firmly place this molecule in an RBBP6/ZBTB38/MCM10 axis that is critical for genome stability in mammalian cells.

Because they are highly susceptible to spontaneous breakage, CFSs are a major cause of genetic instability and have been proposed to have a causal role in different types of cancer (Debatisse et al., 2012). In this context, it is noteworthy that both RBBP6 and ZBTB38 have been connected to cancer. Polymorphisms in ZBTB38 are very tightly linked to the risk of prostate cancer (Kote-Jarai et al., 2011). We speculate that this might be due to the role of ZBTB38 in controlling replication and genome stability via MCM10, and possibly by other genes as well. RBBP6 is highly overexpressed in esophageal cancers (Yoshitake et al., 2004), which are typically p53-negative malignancies with high genetic instability. Based on our data, we hypothesize that RBBP6 deregulation in cancer might contribute to the observed genome instability, and that the effect of RBBP6 in these tumors could be mediated, at least in part, by its action on ZBTB38.

EXPERIMENTAL PROCEDURES

Plasmids

The plasmids used in this work are listed in Table S1.

ChIP and Quantitative PCR

After preclearing with protein A sepharose beads (Millipore) for 1 hr, the chromatin from an equivalent of 5 × 10^7 HeLa cells was used for IP with a ZBTB38

(B) Expression of *MCM10*, but not of other replication genes (i.e., MCM3 and others not shown), is decreased after RBBP6 depletion, increased after ZBTB38 depletion, and normal after combined depletion. qRT-PCR was performed on mRNAs extracted from cells transfected with the indicated siRNAs (average and SD from three biological replicates, with normalization to β2 microglobulin).
(C) MCM10 depletion is not a consequence of DNA damage signaling. The same procedure as in (A) was used, but the experiment was performed in the presence of caffeine, an inhibitor of ATM and ATR signaling.
(D) ZBTB38 represses the *MCM10* promoter in a luciferase transfection assay.
(E) ZBTB38 directly binds the promoter region of *MCM10*. Left panel: schematic description of the genomic region assayed. Right panel: results of ChIP on the endogenous ZBTB38 protein in HeLa cells (average and SD from three experiments). Enrichment values were normalized to an internal control (the GAPDH locus).
(F) ZBTB38 overexpression causes a transcriptional repression of *MCM10*, but not *MCM3*. qRT-PCR analysis in cells transfected with a control plasmid or a ZBTB38 expression plasmid. Expression levels were normalized to an internal control (β2 microglobulin).
(G) The overexpression of ZBTB38 is sufficient to induce MCM10 repression and DNA damage. Western blot analysis of cells transfected with an empty plasmid (Ctrl) or a ZBTB38 expression plasmid. Same extracts as used in Figure 2C.
See also Figure S7.

antibody or immunoglobulin G as a control. After an overnight incubation at 4°C, the beads were washed, eluted in buffer E (25 mM Tris-HCl [pH 7.5], 5 mM EDTA, 0.5% SDS) and crosslinks were reversed at 65°C with proteinase K for 6 hr. The DNA was then purified using the QIAquick PCR purification kit (QIAGEN) and eluted in 100 μl distilled water. Enrichment for a specific DNA sequence was calculated using the comparative Ct method as previously described (Miotto and Struhl, 2008). PCR primer pairs are listed in Table S2.

Immunofluorescence

The cells were fixed for 10 min in 2% paraformaldehyde, permeabilized with 0.5% Triton X-100 at 4°C, and processed for immunofluorescence as previously described (Yamada et al., 2009). When necessary, the cells were treated with the proteasomal inhibitor MG132 at a 20 μM final concentration overnight. Images were processed with ImageJ (http://rsbweb.nih.gov/ij/). ERCC6L/PICH staining on anaphase cells was performed as previously described (Rouzeau et al., 2012). The antibodies used in this work are listed in Table S3.

DNA Combing Analysis

Molecular combing and immunodetection were performed as previously described (Técher et al., 2013).

Gene Expression Analysis

mRNA was isolated using the TRIZOL reagent (Invitrogen) according to a standard protocol. Reverse transcription was performed using the Superscript III reverse transcriptase enzyme (Invitrogen) as recommended by the manufacturer. The primers used for quantitative PCR (qPCR) analysis are available in the PrimerBank database (Spandidos et al., 2010).

Additional experimental procedures are available in Supplemental Experimental Procedures.

SUPPLEMENTAL INFORMATION

Supplemental Information includes Supplemental Experimental Procedures, seven figures, and three tables and can be found with this article online at http://dx.doi.org/10.1016/j.celrep.2014.03.030.

ACKNOWLEDGMENTS

For the gift of reagents, we are grateful to S. Ait-si-ali, R. Everett, R. Fahraeus, E. Matsuda, P. Pasero, O. Sordet, S. Saxena, B. Vogelstein, K. Yoshida, and E. Soutoglou. For insightful comments on the manuscript, we thank G. Almouzni, A. Bardin, C. Francastel, Z. Herceg, E. Julien, S. Khochbin, S. Polo, J. Sage, and M.L. Schmitz. M.C. was supported by a fellowship from the City of Paris. B.M. was supported by the Ligue contre le Cancer (Comité de Paris) and a Marie Curie IRG fellowship (PIRG07-GA-2010-268448). P.A.D. is funded by the Association pour la Recherche contre le Cancer (ARC), Institut National du Cancer (INCa), Groupement des Entreprises Françaises dans la Lutte contre le Cancer (GEFLUC), and Agence Nationale de la Recherche (ANR; ANR-11-LABX-0071 under program ANR-11-IDEX-0005-01). D.P. received financial support from the Medical Research Council of South Africa and the National Research Foundation of South Africa. H.M.S. received funding from the Medical Research Council of South Africa. L.Z.'s lab was supported partially by the National Basic Research Program (2012CB910702 and 2011CB910802) and the National Natural Science Foundation Project (31125010 and 81221004). Work in the lab of M.D. is supported by the INCa, ANR, and ARC.

Received: October 29, 2012
Revised: January 17, 2014
Accepted: March 9, 2014
Published: April 10, 2014

REFERENCES

Aguilera, A., and Gómez-González, B. (2008). Genome instability: a mechanistic view of its causes and consequences. Nat. Rev. Genet. *9*, 204–217.

Arlt, M.F., Ozdemir, A.C., Birkeland, S.R., Wilson, T.E., and Glover, T.W. (2011). Hydroxyurea induces de novo copy number variants in human cells. Proc. Natl. Acad. Sci. USA *108*, 17360–17365.

Balestrini, A., Cosentino, C., Errico, A., Garner, E., and Costanzo, V. (2010). GEMC1 is a TopBP1-interacting protein required for chromosomal DNA replication. Nat. Cell Biol. *12*, 484–491.

Bergoglio, V., Boyer, A.S., Walsh, E., Naim, V., Legube, G., Lee, M.Y., Rey, L., Rosselli, F., Cazaux, C., Eckert, K.A., and Hoffmann, J.S. (2013). DNA synthesis by Pol η promotes fragile site stability by preventing under-replicated DNA in mitosis. J. Cell Biol. *201*, 395–408.

Buchwald, G., van der Stoop, P., Weichenrieder, O., Perrakis, A., van Lohuizen, M., and Sixma, T.K. (2006). Structure and E3-ligase activity of the Ring-Ring complex of polycomb proteins Bmi1 and Ring1b. EMBO J. *25*, 2465–2474.

Burrell, R.A., McGranahan, N., Bartek, J., and Swanton, C. (2013). The causes and consequences of genetic heterogeneity in cancer evolution. Nature *501*, 338–345.

Chan, K.L., and Hickson, I.D. (2009). On the origins of ultra-fine anaphase bridges. Cell Cycle *8*, 3065–3066.

Chen, J., Tang, H., Wu, Z., Zhou, C., Jiang, T., Xue, Y., Huang, G., Yan, D., and Peng, Z. (2013). Overexpression of RBBP6, alone or combined with mutant TP53, is predictive of poor prognosis in colon cancer. PLoS ONE *8*, e66524.

Chibi, M., Meyer, M., Skepu, A., G Rees, D.J., Moolman-Smook, J.C., and Pugh, D.J. (2008). RBBP6 interacts with multifunctional protein YB-1 through its RING finger domain, leading to ubiquitination and proteosomal degradation of YB-1. J. Mol. Biol. *384*, 908–916.

Debatisse, M., Le Tallec, B., Letessier, A., Dutrillaux, B., and Brison, O. (2012). Common fragile sites: mechanisms of instability revisited. Trends Genet. *28*, 22–32.

Domínguez-Kelly, R., Martín, Y., Koundrioukoff, S., Tanenbaum, M.E., Smits, V.A., Medema, R.H., Debatisse, M., and Freire, R. (2011). Wee1 controls genomic stability during replication by regulating the Mus81-Eme1 endonuclease. J. Cell Biol. *194*, 567–579.

Filion, G.J., Zhenilo, S., Salozhin, S., Yamada, D., Prokhortchouk, E., and Defossez, P.A. (2006). A family of human zinc finger proteins that bind methylated DNA and repress transcription. Mol. Cell. Biol. *26*, 169–181.

Fungtammasan, A., Walsh, E., Chiaromonte, F., Eckert, K.A., and Makova, K.D. (2012). A genome-wide analysis of common fragile sites: what features determine chromosomal instability in the human genome? Genome Res. *22*, 993–1005.

Germann, S.M., Oestergaard, V.H., Haas, C., Salis, P., Motegi, A., and Lisby, M. (2011). Dpb11/TopBP1 plays distinct roles in DNA replication, checkpoint response and homologous recombination. DNA Repair (Amst.) *10*, 210–224.

Harrigan, J.A., Belotserkovskaya, R., Coates, J., Dimitrova, D.S., Polo, S.E., Bradshaw, C.R., Fraser, P., and Jackson, S.P. (2011). Replication stress induces 53BP1-containing OPT domains in G1 cells. J. Cell Biol. *193*, 97–108.

Helmrich, A., Ballarino, M., and Tora, L. (2011). Collisions between replication and transcription complexes cause common fragile site instability at the longest human genes. Mol. Cell *44*, 966–977.

Im, J.S., Ki, S.H., Farina, A., Jung, D.S., Hurwitz, J., and Lee, J.K. (2009). Assembly of the Cdc45-Mcm2-7-GINS complex in human cells requires the Ctf4/And-1, RecQL4, and Mcm10 proteins. Proc. Natl. Acad. Sci. USA *106*, 15628–15632.

Jacome, A., and Fernandez-Capetillo, O. (2011). Lac operator repeats generate a traceable fragile site in mammalian cells. EMBO Rep. *12*, 1032–1038.

Kanke, M., Kodama, Y., Takahashi, T.S., Nakagawa, T., and Masukata, H. (2012). Mcm10 plays an essential role in origin DNA unwinding after loading of the CMG components. EMBO J. *31*, 2182–2194.

Kappo, M.A., Ab, E., Hassem, F., Atkinson, R.A., Faro, A., Muleya, V., Mulaudzi, T., Poole, J.O., McKenzie, J.M., Chibi, M., et al. (2012). Solution structure of RING finger-like domain of retinoblastoma-binding protein-6 (RBBP6) suggests it functions as a U-box. J. Biol. Chem. *287*, 7146–7158.

Kim, W., Bennett, E.J., Huttlin, E.L., Guo, A., Li, J., Possemato, A., Sowa, M.E., Rad, R., Rush, J., Comb, M.J., et al. (2011). Systematic and quantitative assessment of the ubiquitin-modified proteome. Mol. Cell *44*, 325–340.

Kote-Jarai, Z., Olama, A.A., Giles, G.G., Severi, G., Schleutker, J., Weischer, M., Campa, D., Riboli, E., Key, T., Gronberg, H., et al.; UK Genetic Prostate Cancer Study Collaborators/British Association of Urological Surgeons' Section of Oncology; UK ProtecT Study Collaborators, The Australian Prostate Cancer BioResource; PRACTICAL Consortium (2011). Seven prostate cancer susceptibility loci identified by a multi-stage genome-wide association study. Nat. Genet. *43*, 785–791.

Koundrioukoff, S., Carignon, S., Técher, H., Letessier, A., Brison, O., and Debatisse, M. (2013). Stepwise activation of the ATR signaling pathway upon increasing replication stress impacts fragile site integrity. PLoS Genet. *9*, e1003643.

Kumagai, A., Shevchenko, A., Shevchenko, A., and Dunphy, W.G. (2010). Treslin collaborates with TopBP1 in triggering the initiation of DNA replication. Cell *140*, 349–359.

Le Tallec, B., Millot, G.A., Blin, M.E., Brison, O., Dutrillaux, B., and Debatisse, M. (2013). Common fragile site profiling in epithelial and erythroid cells reveals that most recurrent cancer deletions lie in fragile sites hosting large genes. Cell Rep. *4*, 420–428.

Letessier, A., Millot, G.A., Koundrioukoff, S., Lachagès, A.M., Vogt, N., Hansen, R.S., Malfoy, B., Brison, O., and Debatisse, M. (2011). Cell-type-specific replication initiation programs set fragility of the FRA3B fragile site. Nature *470*, 120–123.

Li, L., Deng, B., Xing, G., Teng, Y., Tian, C., Cheng, X., Yin, X., Yang, J., Gao, X., Zhu, Y., et al. (2007). PACT is a negative regulator of p53 and essential for cell growth and embryonic development. Proc. Natl. Acad. Sci. USA *104*, 7951–7956.

Lukas, C., Savic, V., Bekker-Jensen, S., Doil, C., Neumann, B., Pedersen, R.S., Grøfte, M., Chan, K.L., Hickson, I.D., Bartek, J., and Lukas, J. (2011). 53BP1 nuclear bodies form around DNA lesions generated by mitotic transmission of chromosomes under replication stress. Nat. Cell Biol. *13*, 243–253.

Mbita, Z., Meyer, M., Skepu, A., Hosie, M., Rees, J., and Dlamini, Z. (2012). De-regulation of the RBBP6 isoform 3/DWNN in human cancers. Mol. Cell. Biochem. *362*, 249–262.

Miotto, B., and Struhl, K. (2008). HBO1 histone acetylase is a coactivator of the replication licensing factor Cdt1. Genes Dev. *22*, 2633–2638.

Motadi, L.R., Bhoola, K.D., and Dlamini, Z. (2011). Expression and function of retinoblastoma binding protein 6 (RBBP6) in human lung cancer. Immunobiology *216*, 1065–1073.

Naim, V., Wilhelm, T., Debatisse, M., and Rosselli, F. (2013). ERCC1 and MUS81-EME1 promote sister chromatid separation by processing late replication intermediates at common fragile sites during mitosis. Nat. Cell Biol. *15*, 1008–1015.

Ozeri-Galai, E., Bester, A.C., and Kerem, B. (2012). The complex basis underlying common fragile site instability in cancer. Trends Genet. *28*, 295–302.

Rouzeau, S., Cordelières, F.P., Buhagiar-Labarchède, G., Hurbain, I., Onclercq-Delic, R., Gemble, S., Magnaghi-Jaulin, L., Jaulin, C., and Amor-Guéret, M. (2012). Bloom's syndrome and PICH helicases cooperate with topoisomerase IIα in centromere disjunction before anaphase. PLoS ONE *7*, e33905.

Sakai, Y., Saijo, M., Coelho, K., Kishino, T., Niikawa, N., and Taya, Y. (1995). cDNA sequence and chromosomal localization of a novel human protein, RBQ-1 (RBBP6), that binds to the retinoblastoma gene product. Genomics *30*, 98–101.

Sasai, N., Matsuda, E., Sarashina, E., Ishida, Y., and Kawaichi, M. (2005). Identification of a novel BTB-zinc finger transcriptional repressor, CIBZ, that interacts with CtBP corepressor. Genes Cells *10*, 871–885.

Sasai, N., Nakao, M., and Defossez, P.A. (2010). Sequence-specific recognition of methylated DNA by human zinc-finger proteins. Nucleic Acids Res. *38*, 5015–5022.

Shi, Y., Di Giammartino, D.C., Taylor, D., Sarkeshik, A., Rice, W.J., Yates, J.R., 3rd, Frank, J., and Manley, J.L. (2009). Molecular architecture of the human pre-mRNA 3′ processing complex. Mol. Cell *33*, 365–376.

Simons, A., Melamed-Bessudo, C., Wolkowicz, R., Sperling, J., Sperling, R., Eisenbach, L., and Rotter, V. (1997). PACT: cloning and characterization of a cellular p53 binding protein that interacts with Rb. Oncogene *14*, 145–155.

Sirbu, B.M., Couch, F.B., Feigerle, J.T., Bhaskara, S., Hiebert, S.W., and Cortez, D. (2011). Analysis of protein dynamics at active, stalled, and collapsed replication forks. Genes Dev. *25*, 1320–1327.

Sognier, M.A., and Hittelman, W.N. (1986). Mitomycin-induced chromatid breaks in HeLa cells: a consequence of incomplete DNA replication. Cancer Res. *46*, 4032–4040.

Soutoglou, E., and Misteli, T. (2008). Activation of the cellular DNA damage response in the absence of DNA lesions. Science *320*, 1507–1510.

Spandidos, A., Wang, X., Wang, H., and Seed, B. (2010). PrimerBank: a resource of human and mouse PCR primer pairs for gene expression detection and quantification. Nucleic Acids Res. *38* (Database issue), D792–D799.

Tanaka, S., Komeda, Y., Umemori, T., Kubota, Y., Takisawa, H., and Araki, H. (2013). Efficient initiation of DNA replication in eukaryotes requires Dpb11/TopBP1-GINS interaction. Mol. Cell. Biol. *33*, 2614–2622.

Taylor, M., Moore, K., Murray, J., Aves, S.J., and Price, C. (2011). Mcm10 interacts with Rad4/Cut5(TopBP1) and its association with origins of DNA replication is dependent on Rad4/Cut5(TopBP1). DNA Repair (Amst.) *10*, 1154–1163.

Técher, H., Koundrioukoff, S., Azar, D., Wilhelm, T., Carignon, S., Brison, O., Debatisse, M., and Le Tallec, B. (2013). Replication dynamics: biases and robustness of DNA fiber analysis. J. Mol. Biol. *425*, 4845–4855.

Thu, Y.M., and Bielinsky, A.K. (2013). Enigmatic roles of Mcm10 in DNA replication. Trends Biochem. Sci. *38*, 184–194.

van Deursen, F., Sengupta, S., De Piccoli, G., Sanchez-Diaz, A., and Labib, K. (2012). Mcm10 associates with the loaded DNA helicase at replication origins and defines a novel step in its activation. EMBO J. *31*, 2195–2206.

Watase, G., Takisawa, H., and Kanemaki, M.T. (2012). Mcm10 plays a role in functioning of the eukaryotic replicative DNA helicase, Cdc45-Mcm-GINS. Curr. Biol. *22*, 343–349.

Wawrousek, K.E., Fortini, B.K., Polaczek, P., Chen, L., Liu, Q., Dunphy, W.G., and Campbell, J.L. (2010). Xenopus DNA2 is a helicase/nuclease that is found in complexes with replication proteins And-1/Ctf4 and Mcm10 and DSB response proteins Nbs1 and ATM. Cell Cycle *9*, 1156–1166.

Yamada, D., Pérez-Torrado, R., Filion, G., Caly, M., Jammart, B., Devignot, V., Sasai, N., Ravassard, P., Mallet, J., Sastre-Garau, X., et al. (2009). The human protein kinase HIPK2 phosphorylates and downregulates the methyl-binding transcription factor ZBTB4. Oncogene *28*, 2535–2544.

Ying, S., Minocherhomji, S., Chan, K.L., Palmai-Pallag, T., Chu, W.K., Wass, T., Mankouri, H.W., Liu, Y., and Hickson, I.D. (2013). MUS81 promotes common fragile site expression. Nat. Cell Biol. *15*, 1001–1007.

Yoshida, K., and Inoue, I. (2004). Expression of MCM10 and TopBP1 is regulated by cell proliferation and UV irradiation via the E2F transcription factor. Oncogene *23*, 6250–6260.

Yoshitake, Y., Nakatsura, T., Monji, M., Senju, S., Matsuyoshi, H., Tsukamoto, H., Hosaka, S., Komori, H., Fukuma, D., Ikuta, Y., et al. (2004). Proliferation potential-related protein, an ideal esophageal cancer antigen for immunotherapy, identified using complementary DNA microarray analysis. Clin. Cancer Res. *10*, 6437–6448.

Zhu, W., Ukomadu, C., Jha, S., Senga, T., Dhar, S.K., Wohlschlegel, J.A., Nutt, L.K., Kornbluth, S., and Dutta, A. (2007). Mcm10 and And-1/CTF4 recruit DNA polymerase alpha to chromatin for initiation of DNA replication. Genes Dev. *21*, 2288–2299.